Biosynthesis of Lipid A in *Escherichia coli*: Identification of UDP-3-*O*-[(*R*)-3-hydroxymyristoyl]-α-D-glucosamine as a Precursor of UDP-N^2,O^3-bis[(*R*)-3-hydroxymyristoyl]-α-D-glucosamine†

Matt S. Anderson,‡ Andrew D. Robertson, Ingolf Macher,§ and Christian R. H. Raetz*
Department of Biochemistry, College of Agricultural and Life Sciences, University of Wisconsin—Madison, Madison, Wisconsin 53706

Received August 5, 1987; Revised Manuscript Received October 27, 1987

ABSTRACT: The lipid A disaccharide of the *Escherichia coli* envelope is synthesized from the two fatty acylated glucosamine derivatives UDP-N^2,O^3-bis[(*R*)-3-hydroxytetradecanoyl]-α-D-glucosamine (UDP-2,3-diacyl-GlcN) and N^2,O^3-bis[(*R*)-3-hydroxytetradecanoyl]-α-D-glucosamine 1-phosphate (2,3-diacyl-GlcN-1-P) [Ray, B. L., Painter, G., & Raetz, C. R. H. (1984) *J. Biol. Chem. 259*, 4852–4859]. We have previously shown that UDP-2,3-diacyl-GlcN is generated in extracts of *E. coli* by fatty acylation of UDP-GlcNAc, giving UDP-3-*O*-[(*R*)-3-hydroxymyristoyl]-GlcNAc as the first intermediate, which is rapidly converted to UDP-2,3-diacyl-GlcN [Anderson, M. S., Bulawa, C. E., & Raetz, C. R. H. (1985) *J. Biol. Chem. 260*, 15536–15541; Anderson, M. S., & Raetz, C. R. H. (1987) *J. Biol. Chem. 262*, 5159–5169]. We now demonstrate a novel enzyme in the cytoplasmic fraction of *E. coli*, capable of deacetylating UDP-3-*O*-[(*R*)-3-hydroxymyristoyl]-GlcNAc to form UDP-3-*O*-[(*R*)-3-hydroxymyristoyl]glucosamine. The covalent structure of the previously undescribed UDP-3-*O*-[(*R*)-3-hydroxymyristoyl]glucosamine intermediate was established by ^{1}H NMR spectroscopy and fast atom bombardment mass spectrometry. This material can be made to accumulate in *E. coli* extracts upon incubation of UDP-3-*O*-[(*R*)-3-hydroxymyristoyl]-GlcNAc in the absence of the fatty acyl donor [(*R*)-3-hydroxymyristoyl]-acyl carrier protein. However, addition of the isolated deacetylation product [UDP-3-*O*-[(*R*)-3-hydroxymyristoyl]glucosamine] back to membrane-free extracts of *E. coli* in the presence of [(*R*)-3-hydroxymyristoyl]-acyl carrier protein results in rapid conversion of this compound into the more hydrophobic products UDP-2,3-diacyl-GlcN, 2,3-diacyl-GlcN-1-P, and *O*-[2-amino-2-deoxy-N^2,O^3-bis[(*R*)-3-hydroxytetradecanoyl]-β-D-glucopyranosyl]-(1→6)-2-amino-2-deoxy-N^2,O^3-bis[(*R*)-3-hydroxytetradecanoyl]-α-D-glucopyranose 1-phosphate (tetraacyldisaccharide-1-P), demonstrating its competency as a precursor. In vitro incubations using [*acetyl*-^{3}H]UDP-3-*O*-[(*R*)-3-hydroxymyristoyl]-GlcNAc confirmed release of the acetyl moiety in this system as acetate, not as some other acetyl derivative. The deacetylation reaction was inhibited by 1 mM *N*-ethylmaleimide, while the subsequent N-acylation reaction was not. Our observations provide strong evidence that UDP-3-*O*-[(*R*)-3-hydroxymyristoyl]glucosamine is a true intermediate in the biosynthesis of UDP-2,3-diacyl-GlcN and lipid A.

The lipid A component of *Escherichia coli* lipopolysaccharide is a β(1→6)-linked glucosamine disaccharide (Figure 1), bearing six fatty acyl moieties and at least two phosphomonoester residues (Raetz, 1986; Rietschel, 1984; Galanos et al., 1977; Hinshaw, 1984; Takayama et al., 1983a,b; Rietschel et al., 1983; Imoto et al., 1983; Qureshi et al., 1983). Lipid A has been implicated as the causative agent in Gram-negative shock (Hinshaw, 1984; Rietschel, 1984), and it exerts diverse pathophysiological effects, including pyrogenicity, stimulation of B-lymphocyte proliferation, and activation of macrophages (Galanos et al., 1979; Morrison & Ryan, 1979). While these phenomena have been appreciated for many years, the actual covalent structure of lipid A (Figure 1) was unknown prior to 1983 (Strain et al., 1983; Takayama et al., 1983a,b; Rietschel et al., 1983; Imoto et al., 1983; Qureshi et al., 1983; Rietschel, 1984; Raetz, 1986).

Evidence for the early stages of lipid A biosynthesis (Figure 1) was provided by the discovery of two monosaccharide precursors of lipid A that accumulate in mutants defective in the *lpxB* gene (Takayama et al., 1983a; Bulawa & Raetz, 1984a). This locus (Ray et al., 1984; Crowell et al., 1986) encodes the lipid A disaccharide synthase, an enzyme that utilizes 2,3-diacyl-GlcN-1-P[1] and UDP-2,3-diacyl-GlcN in the synthesis of a β(1→6)-linked tetraacyldisaccharide 1-phosphate intermediate (Figure 1) (Ray et al., 1984). These monosaccharide precursors accumulate to high levels in such mutants (Takayama et al., 1983a; Bulawa & Raetz, 1984a) and were shown by Anderson and Raetz (1987) to be formed from UDP-GlcNAc by two successive acylations of the glucosamine

†This work was supported by National Institutes of Health Grant DK 19551 to C.R.H.R.

*Address correspondence to this author at Merck, Sharp and Dohme Research Laboratories, P.O. Box 2000, Rahway, NJ 07065.
‡Present address: Department of Chemistry, Henry Eyring Building, The University of Utah, Salt Lake City, UT 84112.
§Present address: Sandoz Forschungsinstitut, Vienna, Austria.

[1] Abbreviations: KDO, 3-deoxy-D-*manno*-octulosonate; UDP-3-*O*-[(*R*)-3-hydroxymyristoyl]-GlcNAc, UDP-*N*-acetyl-3-*O*-[(*R*)-3-hydroxytetradecanoyl]-α-D-glucosamine; 2,3-diacylglucosamine-1-P or 2,3-diacyl-GlcN-1-P or lipid X, N^2,O^3-bis[(*R*)-3-hydroxytetradecanoyl]-α-D-glucosamine 1-phosphate; UDP-2,3-diacyl-GlcN, UDP-N^2,O^3-bis[(*R*)-3-hydroxytetradecanoyl]-α-D-glucosamine; tetraacyldisaccharide 1-phosphate or tetraacyldisaccharide-1-P, *O*-[2-amino-2-deoxy-N^2,O^3-bis[(*R*)-3-hydroxytetradecanoyl]-β-D-glucopyranosyl]-(1→6)-2-amino-2-deoxy-N^2,O^3-bis[(*R*)-3-hydroxytetradecanoyl]-α-D-glucopyranose 1-phosphate; PEI, poly(ethylenimine); FAB, fast atom bombardment; HEPES, *N*-(2-hydroxyethyl)piperazine-*N*′-2-ethanesulfonic acid; Bis-Tris, 2-[bis(2-hydroxyethyl)amino]-2-(hydroxymethyl)propane-1,3-diol; ACP, acyl carrier protein; HPLC, high-pressure liquid chromatography; NMP, nucleotide monophosphate; NDP-GlcNAc, nucleotide diphosphate *N*-acetylglucosamine; BSA, bovine serum albumin; EDTA, ethylenediaminetetraacetic acid.

0006-2960/88/0427-1908$01.50/0

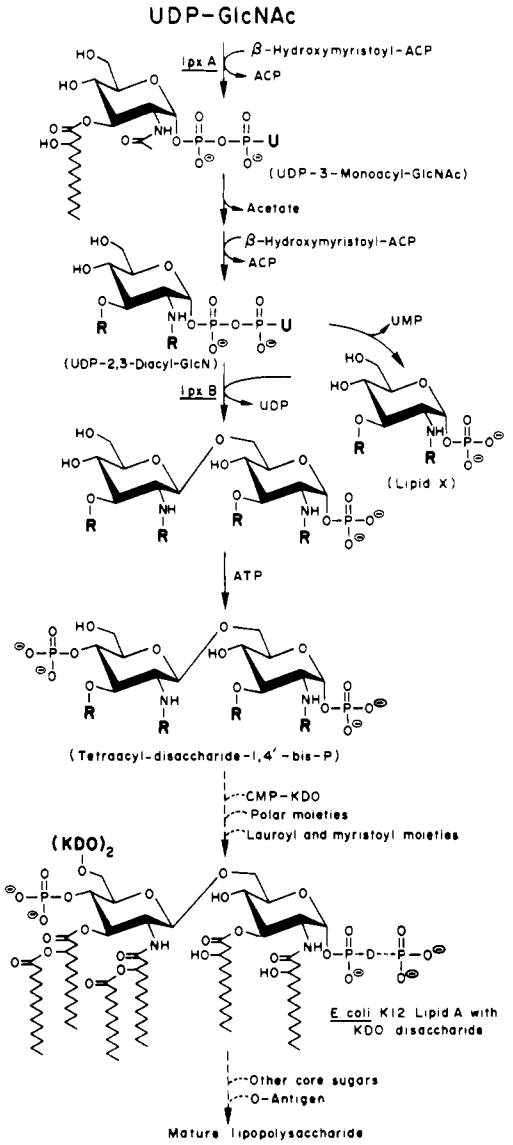

FIGURE 1: Pathway for the biosynthesis of lipid A in *E. coli*. Synthesis begins with the fatty acylation of UDP-GlcNAc at position 3 of the glucosamine ring (Anderson & Raetz, 1987). The resulting UDP-3-*O*-[(*R*)-3-hydroxymyristoyl]-GlcNAc then undergoes deacetylation followed by N-acylation with another (*R*)-3-hydroxymyristoyl group, as documented in the present study. Evidence for all the other reactions has been presented previously (Raetz, 1986). In the figure, R represents an (*R*)-3-hydroxymyristoyl moiety, U represents uridine, and KDO represents 3-deoxy-D-*manno*-octulosonate.

ring. Initially, UDP-3-*O*-[(*R*)-3-hydroxymyristoyl]-GlcNAc is formed in a reaction dependent upon [(*R*)-3-hydroxymyristoyl]-acyl carrier protein and is the first intermediate of the pathway, while 2,3-diacyl-GlcN-1-P (also termed lipid X) is formed by the hydrolysis of the pyrophosphate linkage of UDP-2,3-diacyl-GlcN (Anderson & Raetz, 1987) (Figure 1).

The second fatty acylation of UDP-GlcNAc (Figure 1) must somehow be preceded by removal of the acetyl moiety. Although the second acylation proceeds very rapidly when UDP-GlcNAc and [(*R*)-3-hydroxymyristoyl]-ACP are incubated together with a crude extract of *E. coli*, nothing is known concerning the enzymatic course of this process. We now present evidence that the formation of UDP-2,3-diacyl-GlcN involves the initial removal of the acetyl moiety from UDP-3-*O*-[(*R*)-3-hydroxymyristoyl]-GlcNAc to yield UDP-3-*O*-[(*R*)-3-hydroxymyristoyl]glucosamine, a metabolite that does not accumulate under ordinary conditions (Anderson & Raetz, 1987). This material, after purification, can then be rapidly acylated at the free amino group when incubated with [(*R*)-3-hydroxymyristoyl]-ACP and *E. coli* extract to yield UDP-2,3-diacyl-GlcN. Demonstration of these enzymes completes the proof for the existence of all the early metabolic steps shown in Figure 1 and opens the way for mechanistic and pharmacologic studies on this intriguing part of *E. coli* metabolism.

EXPERIMENTAL PROCEDURES

Materials. [γ-^{32}P]ATP and [^{3}H]acetic anhydride were obtained from New England Nuclear. Acyl carrier protein (ACP) was isolated from *E. coli* strain W3106 by the method of Rock and Cronan (1983). Silica gel 60 thin-layer plates (0.25 mm) and PEI–cellulose F thin-layer plates (0.1 mm) were products of E. Merck, Darmstadt, Germany.

Bacterial Strains. All strains used were derivatives of *E. coli* K-12. Most assays were performed with extracts of JB1104, which contains a *Tn10* insertion in the structural gene for cytidine 5′-diphosphate diglyceride hydrolase (CDP-diglyceride hydrolase) (Bulawa & Raetz, 1984b). This hydrolase has been shown to cleave the pyrophosphate bridge of both UDP-3-*O*-acyl-GlcNAc and UDP-2,3-diacyl-GlcN to yield UMP and the corresponding acylglucosamine 1-phosphate (Bulawa & Raetz, 1984a). Strains lacking this hydrolase were used to avoid destruction of these compounds by this route. Strain W3106 was obtained from the *E. coli* Genetic Stock Center, Yale University, New Haven, CT.

Preparation of E. coli Cell Extracts. Cell extracts were made from strain JB1104 as described previously (Anderson & Raetz, 1987). Unless otherwise indicated, all assays were performed on membrane-free cell supernatants. Protein concentrations were determined by the method of Peterson (1977) with BSA as the standard.

Preparation of Acyl Donors and Radiolabeled Substrates. [(*R*)-3-Hydroxymyristoyl]-ACP was prepared as described by Anderson and Raetz (1987). [β-^{32}P]UDP-GlcNAc, [β-^{32}P]-UDP-3-*O*-[(*R*)-3-hydroxymyristoyl]GlcNAc, and [*acetyl*-^{3}H]UDP-GlcNAc were prepared as described previously (Lang & Kornfeld, 1984; Anderson & Raetz, 1987). [*acetyl*-^{3}H]UDP-3-*O*-[(*R*)-3-hydroxymyristoyl]-GlcNAc was prepared from [*acetyl*-^{3}H]UDP-GlcNAc, by using the same conditions described for the synthesis of the ^{32}P-labeled material.

Chemical Synthesis of UDP-3-O-[(R)-3-hydroxymyristoyl]-GlcNAc. Synthetic UDP-3-*O*-[(*R*)-3-hydroxymyristoyl]-GlcNAc was prepared by the method shown in Scheme I. To a solution of 4,6-*O*-benzylidene-GlcNAc (**1**; Roth & Pigman, 1960) (5.17 g, 16.7 mmol) and imidazole (3.41 g, 50 mmol) in *N*,*N*-dimethylformamide (300 mL) was added *tert*-butyldimethylsilyl chloride (6.3 g, 41.8 mmol), and the mixture was kept for 6 h at 60 °C. Then the solvent was evaporated and the residue partitioned between dichloromethane and water. The organic phase was dried ($MgSO_4$) and evaporated. Column chromatography [in toluene/ethyl acetate (5:1 v/v) on Merck-Lichroprep, silica gel, 40–63 μm] of the residue gave bis(silyl) derivative **2** in 83% yield. Compound **2** was quantitatively 1-O-desilylated by dissolving it in dry tetrahydrofuran and adding 1 equiv of tetrabutylammonium fluoride at −40 °C. The reaction was quenched after 10 min by the addition of methanol. The solution was concentrated, and the residue dissolved in dichloromethane, extracted with water, dried ($MgSO_4$), and concentrated again. 3-*O*-Monosilyl derivative **3**, obtained as a mixture of anomers, was dibenzylphosphorylated according to a modified method of Inage et al. (1982) (Macher, 1987). To a −40 °C cold

Scheme I

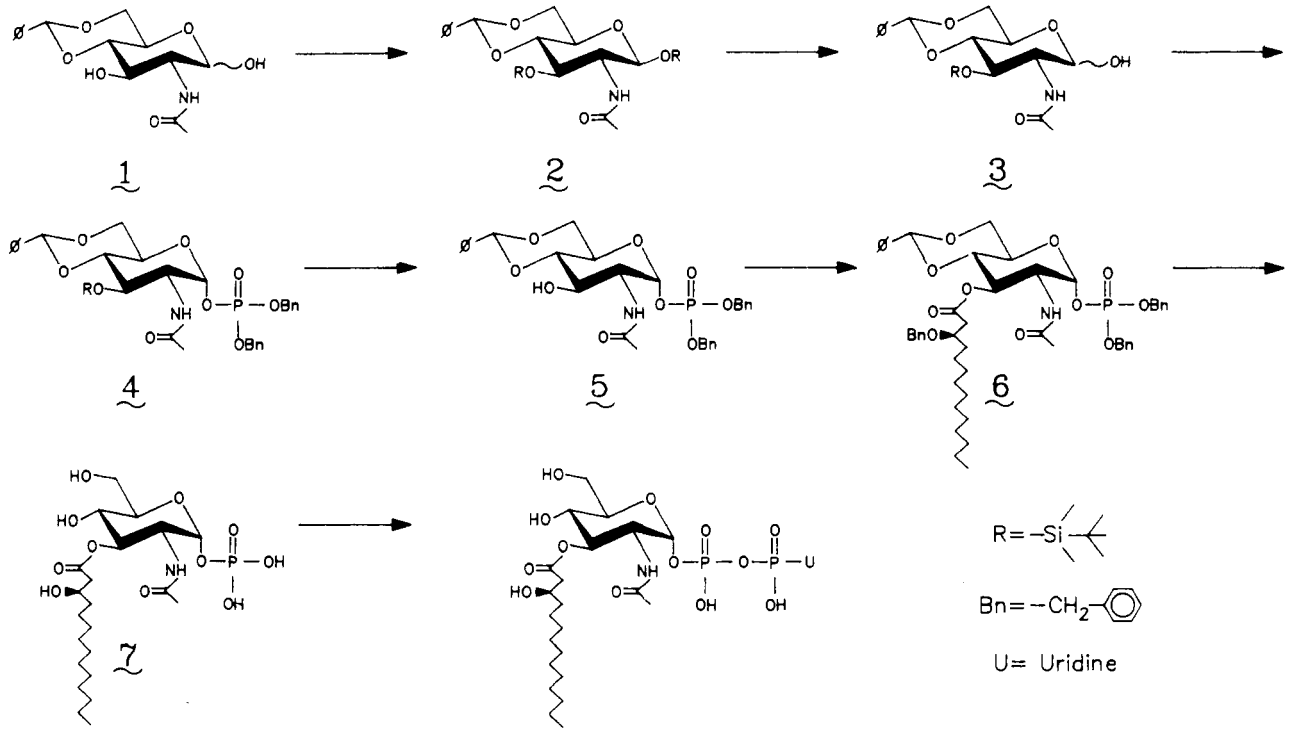

solution of **3** (2.83 g, 6.7 mmol) in dry tetrahydrofuran (500 mL) were added *n*-butyllithium in hexane (5 mL, 1.6 M) and, 5 min later, dibenzyl chlorophosphonate (Kenner et al., 1952) (8 mmol in 8 mL of benzene). After 10 min, acetic acid (0.2 mL) was added. The mixture was concentrated, and the residue was chromatographed over silica gel [toluene/ethyl acetate (1:1 v/v)] to give the 1-α-phosphate derivative **4** in 51% yield. The 3-hydroxy derivative **5** was obtained in quantitative yield by treatment of a solution of **4** in tetrahydrofuran with 1 equiv of tetrabutylammonium fluoride at 0 °C and workup as described for the preparation of **3**. A solution of **5** (3.5 g, 6.2 mmol), (*R*)-3-(benzyloxy)myristic acid (2.1 g, 6.3 mmol) and 4-(dimethylamino)pyridine (50 mg) in dry dichloromethane (15 mL) was chilled with ice, and then dicyclohexylcarbodiimide (1.32 g, 6.3 mmol) was added. After 2 h the mixture was filtered and the filtrate evaporated. The residue was chromatographed twice over silica gel, first in dichloromethane/methanol (30:1 v/v) and then in toluene/ethyl acetate (1:1 v/v) to give the fully protected 3-*O*-acyl-GlcNAc-1-P **6** in 67% yield. A solution of **6** (250 mg, 0.28 mmol) in 20 mL of tetrahydrofuran/water (9:1 v/v) was hydrogenated for 2 h over 10% Pd/C (190 mg). The catalyst was filtered off, and the filtrate was lyophilized to give a 78% yield of **7**. Reaction of **7** with UMP-morpholidate in pyridine and chromatographic workup was performed according to the method described by Bulawa and Raetz (1984a). UDP-3-*O*-[(*R*)-3-hydroxymyristoyl]-GlcNAc was obtained as a uniform tris(hydroxymethyl)aminomethane (Tris) salt by treatment of a tetrahydrofuran/water (1:1 v/v) solution with Dowex AG 50 WX8 "Tris" form and lyophilization. For final purification, a solution of the lyophilizate in methanol was chromatographed over Sephadex LH-20, using methanol.

Enzymatic Deacetylation of UDP-3-O-[(R)-3-hydroxymyristoyl]-GlcNAc. Deacetylation of UDP-3-*O*-[(*R*)-3-hydroxymyristoyl]-GlcNAc was assayed by incubating 25 μM [β-^{32}P]UDP-3-*O*-[(*R*)-3-hydroxymyristoyl]-GlcNAc in either 40 mM HEPES, pH 8.0, or 40 mM ammonium acetate, pH 5.5, with 3.0 mg/mL membrane-free supernatant at 30 °C in a final volume of 20 μL. Such extracts contain a lipase activity that removes the (*R*)-3-hydroxymyristoyl moiety from the 3-position hydroxyl of both UDP-3-*O*-[(*R*)-3-hydroxymyristoyl]-GlcNAc (Anderson & Raetz, 1987) and UDP-3-*O*-[(*R*)-3-hydroxymyristoyl]-GlcN. This lipase was found to be active at pH 8.0 but virtually inactive at pH 5.5, whereas the deacetylase activity was relatively unaffected. At various times, 2 μL of the incubation mixture was taken and spotted directly onto PEI–cellulose plates. The plates were dried under a cool stream of air, washed for 5 min with MeOH in a baking dish, dried, and developed in MeOH/0.2 M guanidine hydrochloride (44:56 v/v). The plates were dried and autoradiographed to locate products.

Large-Scale Enzymatic Synthesis of UDP-3-O-[(R)-3-hydroxymyristoyl]-GlcN. Several milligrams of UDP-3-*O*-[(*R*)-3-hydroxymyristoyl]-GlcN were prepared for the purpose of ^{1}H NMR analysis from chemically synthesized UDP-3-*O*-[(*R*)-3-hydroxymyristoyl]-GlcNAc in an enzymatic incubation. Reaction mixtures contained 400 μM UDP-3-*O*-[(*R*)-3-hydroxymyristoyl]-GlcNAc, 40 mM ammonium acetate, pH 5.5, and 4 mg/mL of JB1104 membrane-free supernatant in a volume of 3 mL. Five such reactions were carried out simultaneously. Incubations were performed at 30 °C for 20 min, after which an additional 4 mg/mL of protein was added and the incubation allowed to proceed an additional 20 min. At 40 min total reaction time, the mixtures were made 80% in ethanol and put on ice for 15 min. The debris was removed by centrifugation, and the supernatants were pooled. The pooled material was passed over a silica Sep-Pak (Waters Associates) that had been preequilibrated with 80% ethanol in water. The Sep-Pak run-through was collected and the column eluted with 2 bed volumes of 80% ethanol. The run-through and first fraction (found to contain all radiolabeled materials) were pooled, reduced to one-third volume on a vacuum pump, and lyophilized to a powder. The residue was redissolved in 0.05% ammonium acetate, pH 5.5, containing 1 mM EDTA. After 20 min at room temperature, the material was prefiltered and subjected to HPLC. The separation of UDP-3-*O*-[(*R*)-3-hydroxymyristoyl]-GlcN from contaminating materials was achieved by using the 0.05%

ammonium acetate, pH 5.4, C18 reverse-phase system described by Anderson and Raetz (1987) for the purification of UDP-3-*O*-[(*R*)-3-hydroxymyristoyl]-GlcNAc. UDP-3-*O*-[(*R*)-3-hydroxymyristoyl]-GlcNAc and UDP-3-*O*-[(*R*)-3-hydroxymyristoyl]-GlcN elute in this system in approximately 37% and 44% acetonitrile, respectively. As the desired material eluted from the column, it was titrated with 0.1 volume of 10 mM sodium phosphate, pH 6.0, concentrated under reduced pressure, and lyophilized. The sample was D_2O exchanged twice and frozen at −80 °C until examined by ^1H NMR spectroscopy.

^1H NMR Spectroscopy. All ^1H NMR spectra were obtained on a Bruker AM-400 spectrometer operating at 400.13 MHz and equipped with an Aspect 3000 computer. The samples were analyzed in 0.5 mL of D_2O at pD 6.0. Sample temperature was maintained at 21 °C throughout the experiments, unless otherwise indicated. Data for one-dimensional spectra were obtained with a single-pulse experiment. The carrier frequency was placed in the middle of the spectrum and the spectral width was typically 3400–3600 Hz. Each experiment was the sum of 128 transients collected in 8K data points. Before Fourier transformation, the data were weighted by an exponential decay function, with a line-broadening factor of 0.5–1.5 Hz. Data for magnitude-calculated $^1H\{^1H\}$ chemical shift correlation spectroscopy (COSY) were acquired with a 90°–t_1–60°–acquisition pulse sequence to maximize cross-peak intensity (Bax & Freeman, 1981) and with phase cycling for quadrature detection and suppression of axial and P-type peaks (Wider et al., 1984). Pure-absorption COSY data were acquired by using time-proportional phase incrementation (Marion & Wüthrich, 1983). In each experiment, t_1 was incremented from 0.003 to 37 ms in 256 steps, each block being 2K data points in size. The t_1 data were zero-filled to 1K points, and both t_2 and t_1 data were multiplied by sine bells prior to Fourier transformation. All COSY data are presented as magnitude-calculated spectra. Chemical shifts are expressed in parts per million (ppm) downfield from tetramethylsilane, added as an internal standard.

Preparation of [β-^{32}P]UDP-3-O-[(R)-3-hydroxymyristoyl]-GlcN. Samples of [β-^{32}P]UDP-3-*O*-[(*R*)-3-hydroxymyristoyl]-GlcN were prepared enzymatically from [β-^{32}P]UDP-3-*O*-[(*R*)-3-hydroxymyristoyl]-GlcNAc as follows. Reaction mixtures contained 20–40 μM [β-^{32}P]UDP-3-*O*-[(*R*)-3-hydroxymyristoyl]-GlcNAc (specific radioactivity 2×10^6 cpm/nmol), 40 mM Bis-Tris, pH 5.5, and 5 mg/mL JB1104 membrane-free supernatant in a final volume of 50 μL. Reactions were performed for 30 min at 30 °C. At the end of this time, the reaction was diluted with 750 μL of 0.05% ammonium acetate, pH 5.4, prefiltered with a 0.2-μm filter, and fractionated by the C18 reverse-phase HPLC system described above for the large-scale preparation of this compound.

Enzymatic Acylation of UDP-3-O-[(R)-3-hydroxymyristoyl]-GlcN To Form UDP-2,3-diacyl-GlcN. Competency of UDP-3-*O*-[(*R*)-3-hydroxymyristoyl]-GlcN as an intermediate in the synthesis of UDP-2,3-diacyl-GlcN was demonstrated by incubating 3.2 μM [β-^{32}P]UDP-3-*O*-[(*R*)-3-hydroxymyristoyl]-GlcN with 40 mM HEPES, pH 8.0, 100 μM [(*R*)-3-hydroxymyristoyl]-ACP, and 0.8 mg/mL membrane-free supernatant at 30 °C in a final volume of 20 μL. An identical reaction was performed with 0.8 mg/mL membrane-free supernatant which had been preincubated with 1 mM *N*-ethylmaleimide for 30 min at 0 °C. At various times 2-μL aliquots of these reaction mixtures were spotted directly onto silica thin-layer plates with chemical standards of UDP-2,3-diacyl-GlcN, 2,3-diacyl-GlcN-1-P, and tetraacyldisaccharide-1-P. The plates were developed in chloroform/methanol/water/acetic acid (25:15:4:2 v/v), dried, and autoradiographed overnight. Standards were located as described previously (Anderson & Raetz, 1987).

Analysis of [acetyl-^{3}H]UDP-3-O-[(R)-3-hydroxymyristoyl]-GlcNAc Metabolism. Release of acetate from UDP-3-*O*-[(*R*)-3-hydroxymyristoyl]-GlcNAc during the formation of UDP-3-*O*-[(*R*)-3-hydroxymyristoyl]-GlcN was observed directly by using [*acetyl*-^{3}H]UDP-3-*O*-[(*R*)-3-hydroxymyristoyl]-GlcNAc, prepared as described above. Samples of [*acetyl*-^{3}H]UDP-3-*O*-[(*R*)-3-hydroxymyristoyl]-GlcNAc (specific radioactivity 4200 cpm/nmol) were incubated at 25 μM with 40 mM Bis-Tris, pH 6.0, and 5 mg/mL JB1104 membrane-free extract at 30 °C in a final volume of 560 μL. At various times, 100-μL samples were removed and rapidly frozen in liquid nitrogen. Samples were kept frozen in this manner prior to analysis in order to avoid further metabolism or volatilization of any labeled metabolites. For analysis, samples were diluted with 750 μL of 0.05% ammonium acetate, pH 5.4, prefiltered, and analyzed by C18 reverse-phase HPLC as described for the large-scale preparation of UDP-3-*O*-[(*R*)-3-hydroxymyristoyl]-GlcN. One-milliliter fractions were collected, and 0.5 mL of each fraction was counted in 10 mL of 3a70B liquid scintillation cocktail (RPI Products).

RESULTS

Metabolism of UDP-3-O-[(R)-3-hydroxymyristoyl]-GlcNAc in E. coli Extracts. We have previously shown that membrane-free extracts of *E. coli* contain a specific UDP-GlcNAc acyltransferase that transfers an (*R*)-3-hydroxymyristoyl moiety from [(*R*)-3-hydroxymyristoyl]-ACP to UDP-GlcNAc, forming UDP-3-*O*-[(*R*)-3-hydroxymyristoyl]-GlcNAc (Anderson & Raetz, 1987). During our studies of this process, we discovered that [β-^{32}P]UDP-3-*O*-[(*R*)-3-hydroxymyristoyl]-GlcNAc, when incubated by itself in an enzymatic extract at pH 8.0 in the absence of a fatty acyl donor (see Experimental Procedures), yielded three new products. A typical time course is shown in Figure 2, lanes 2–5. As expected, one of these products was [β-^{32}P]UDP-GlcNAc, formed by the action of a lipase that removes the fatty acid at position 3 (Anderson & Raetz, 1987). Unexpectedly, a second metabolite migrated with carrier UDP-glucosamine (Figure 2). This material could not have been formed by deacetylation of [β-^{32}P]UDP-GlcNAc, since extracts of strain JB1104 cannot carry out this reaction (data not shown). UDP-GlcN formation suggested the presence of [β-^{32}P]UDP-3-*O*-[(*R*)-3-hydroxymyristoyl]-GlcN in these reaction mixtures, which could presumably be attacked by the lipase to yield [β-^{32}P]UDP-GlcN. The third metabolite formed in this incubation (Figure 2, uppermost spot), tentatively identified as [β-^{32}P]UDP-3-*O*-[(*R*)-3-hydroxymyristoyl]-GlcN, did not accumulate to very high levels.

In searching for conditions that minimized the destruction of the 3-*O*-acylated materials and that optimized the yield of the putative [β-^{32}P]UDP-3-*O*-[(*R*)-3-hydroxymyristoyl]-GlcN, we discovered that the lipase was much less active at pH 5.5, whereas the deacetylating activity was relatively unaffected (Figure 2, lanes 8–11). Little or no UDP-3-*O*-[(*R*)-3-hydroxymyristoyl]-GlcNAc decomposition occurred at either pH in the absence of enzyme (Figure 2, lanes 7 and 13). Interestingly, both the lipase and the deacetylase were inhibitable by preincubation of the extract with 1 mM *N*-ethylmaleimide (Figure 2, lanes 6 and 12). Inhibition of the deacetylase was complete.

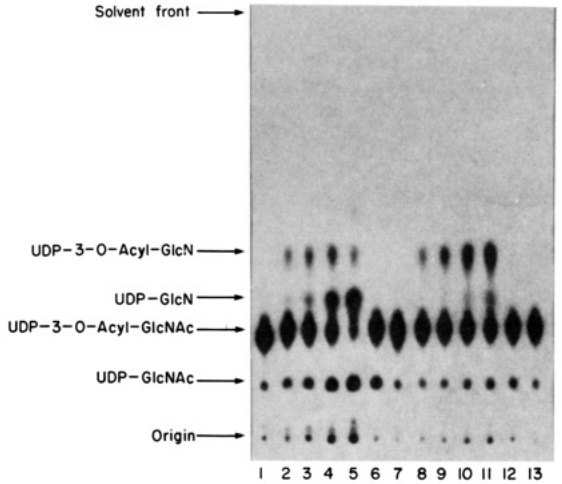

FIGURE 2: Metabolism of [β-^{32}P]UDP-3-*O*-[(*R*)-3-hydroxymyristoyl]-GlcNAc in an *E. coli* extract. This figure is an autoradiograph of a PEI–cellulose thin-layer chromatogram developed in 0.2 M guanidine hydrochloride/methanol (50:50 v/v). The origin, solvent front, and mobilities of various standards are indicated. With the exceptions noted, each reaction mixture contained 25 μM [β-^{32}P]UDP-3-*O*-[(*R*)-3-hydroxymyristoyl]-GlcNAc (2×10^6 cpm/nmol), 40 mM buffer, and 3 mg/mL membrane-free supernatant from strain JB1104 (*cdh*::*Tn10*, *lpxB*$^+$, *lpxA*$^+$), prepared as described under Experimental Procedures. Samples of each reaction mixture (2 μL) were spotted directly onto the plate at the times indicated. Lane 1, [β-^{32}P]UDP-3-*O*-[(*R*)-3-hydroxymyristoyl]-GlcNAc substrate spotted directly onto the plate. Lanes 2–5, portions of a complete reaction mixture spotted at 2, 5, 15, or 30 min, respectively, with 40 mM HEPES, pH 8.0, as the buffer. Lane 6, identical with lane 5 but with a 30-min preincubation of the extract at 0 °C in the presence of 1 mM *N*-ethylmaleimide. Lane 7, identical with lane 5 but with no added extract. Lanes 8–11, 2-, 5-, 15- and 30-min time points, respectively, with 40 mM ammonium acetate, pH 5.5, as the buffer. Lane 12, identical with lane 11 but with a 30-min preincubation of the extract at 0 °C with 1 mM *N*-ethylmaleimide. Lane 13, identical with lane 11 but with no added extract.

Alkali Stability of the Putative UDP-3-O-[(R)-3-hydroxymyristoyl]glucosamine. In order to demonstrate the presence of an ester-linked fatty acid in the putative [β-^{32}P]UDP-3-*O*-[(*R*)-3-hydroxymyristoyl]-GlcN, we isolated a radiolabeled sample of this material for hydrolytic analysis as described under Experimental Procedures. As shown in Figure 3 (panel A, lane 3), this compound migrates with the starting material, [β-^{32}P]UDP-3-*O*-[(*R*)-3-hydroxymyristoyl]-GlcNAc, during silica thin-layer chromatography (panel A, lane 1) but is easily separable during PEI–cellulose thin-layer chromatography (panel B, lanes 1 and 3). Next, both the starting material and the putative [β-^{32}P]UDP-3-*O*-[(*R*)-3-hydroxymyristoyl]-GlcN were treated with mild base, which breaks ester bonds, but not amide or phosphodiester linkages (Bulawa & Raetz, 1984a). Analysis of the hydrolyzed material by silica thin-layer chromatography shows that the radioactive hydrolysis product(s) of both compounds remained on the origin (panel A, lanes 2 and 4), indicating the presence of an ester-linked fatty acyl moiety in the putative UDP-3-*O*-[(*R*)-3-hydroxymyristoyl]-GlcN. Analysis of these mild alkaline hydrolysis products by PEI–cellulose chromatography revealed that the deacylated product derived from the starting material is the expected [β-^{32}P]UDP-GlcNAc (panel B, lane 2), whereas the putative [β-^{32}P]UDP-3-*O*-[(*R*)-3-hydroxymyristoyl]-GlcN is converted to [β-^{32}P]UDP-GlcN (panel B, lane 4).

^{1}H NMR Spectroscopy of UDP-3-O-[(R)-3-hydroxymyristoyl]glucosamine. The "large-scale" enzymatically synthesized sample of the putative UDP-3-*O*-[(*R*)-3-hydroxymyristoyl]-GlcN (see Experimental Procedures) was

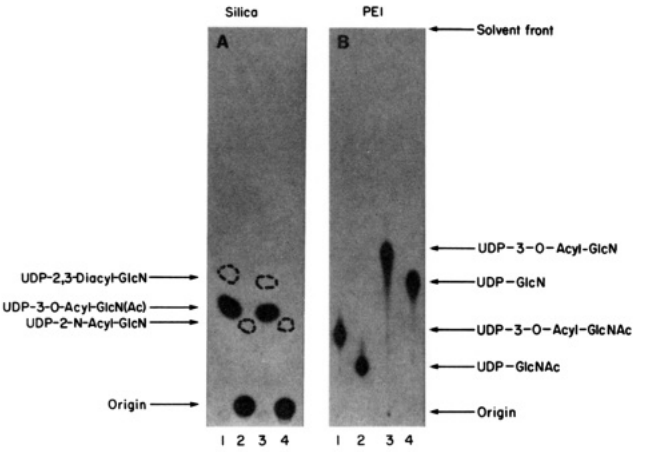

FIGURE 3: Mild alkaline hydrolysis of [β-^{32}P]UDP-3-*O*-[(*R*)-3-hydroxymyristoyl]-GlcNAc and of the putative [β-^{32}P]UDP-3-*O*-[(*R*)-3-hydroxymyristoyl]-GlcN. Samples of [β-^{32}P]UDP-3-*O*-[(*R*)-3-hydroxymyristoyl]-GlcNAc and of [β-^{32}P]UDP-3-*O*-[(*R*)-3-hydroxymyristoyl]-GlcN, prepared as described under Experimental Procedures, were dissolved in 100 μL of MeOH/water (1:1 v/v), together with 40 nmol of carrier UDP-2,3-diacyl-GlcN. Five-microliter aliquots of each solution were spotted onto a silica gel 60 F-254 plate (panel A, lanes 1 and 3, respectively). Two-microliter aliquots of each were also spotted onto a PEI–cellulose F-254 plate (panel B, lanes 1 and 3, respectively). The remaining mixtures were then made alkaline with 4 μL of 1 N NaOH and incubated at room temperature for 30 min. Next, the reactions were neutralized by addition of 4 μL of 1 M Tris-HCl. Five-microliter portions of each sample were then spotted onto silica (panel A, lanes 2 and 4, respectively). Two-microliter portions of these samples were also spotted onto PEI–cellulose (panel B, lanes 2 and 4, respectively). The PEI–cellulose plate was also spotted with 15 nmol of carrier UDP-GlcNAc and UDP-glucosamine in each of lanes 1–4. The silica plate was developed in chloroform/methanol/water/acetic acid (25:15:4:2 v/v), and following autoradiography, the standards were visualized by fluorescence quenching. The positions of the standards, UDP-2,3-diacyl-GlcN (panel A, lanes 1 and 3) and its base hydrolysis product UDP-2-*N*-[(*R*)-3-hydroxymyristoyl]glucosamine (panel A, lanes 2 and 4), are indicated by dashed circles. The PEI–cellulose plate was washed for 15 min in MeOH, dried, and developed in MeOH/0.2 M guanidine hydrochloride (44:56 v/v). Following autoradiography to locate ^{32}P-labeled substances, the carrier sugar nucleotides were visualized by fluorescence quenching. The positions of the radiolabeled substances, as well as UDP-GlcNAc and UDP-GlcN standards, are indicated for each panel.

initially examined by using a 1-pulse one-dimensional ^{1}H NMR experiment. The spectrum thus obtained is shown in the upper panel of Figure 4 and is compared with a similarly obtained spectrum of the starting material, chemically synthesized UDP-3-*O*-[(*R*)-3-hydroxymyristoyl]-GlcNAc (Figure 4, lower panel). Comparison of these spectra reveals the retention of a single (*R*)-3-hydroxymyristoyl group in the new product as evidenced by the fatty acyl methyl triplet at 0.71 ppm (HM-14), the fatty acyl methylene envelope centered at 1.12 ppm, and the C-4 (HM-4) methylene group at 1.37 ppm. The C-3 (HM-3) proton at the site of acyl hydroxylation is also evident at 3.95 ppm. The resonances at 7.8 and 5.8 ppm, arising from the uridine base, are also retained. Importantly, the acetate singlet found at 1.87 ppm in the starting material is absent from the UDP-3-*O*-[(*R*)-3-hydroxymyristoyl]-GlcN spectrum. Several broad resonances (designated X) are not coupled to any of the other uridine, fatty acyl, or glucosamine resonances in the spectrum and are presumed to be impurities from the crude cell extract used as the source of the deacetylase.

An expansion of the spectrum of the product in the region from 2.2 to 6.0 ppm is shown in the top tracing (designated T_0) of Figure 5. To determine the interrelationships of these signals and the positioning of the (*R*)-3-hydroxymyristoyl

Table I: Summary of Chemical Shifts (ppm) and Coupling Constants (Hz) of Relevant Glucosamine Ring Protons of Substrate UDP-3-*O*-[(*R*)-3-hydroxymyristoyl]-GlcNAc, Enzymatic Product UDP-3-*O*-[(*R*)-3-hydroxymyristoyl]-GlcN, and Corresponding Nonenzymatically Formed UDP-6-*O*-[(*R*)-3-hydroxymyristoyl]-GlcNAc and UDP-6-*O*-[(*R*)-3-hydroxymyristoyl]-GlcN

	H-1	H-2	H-3	H-4	H-5	H-$6_{a,b}$[a]
UDP-3-*O*-[(*R*)-3-hydroxymyristoyl]-GlcNAc	5.42 $J_{1,2}$ = 3.4 $J_{1,P}$ = 7	4.05 $J_{2,3}$ = 10.5 $J_{2,P}$ = 2.8	5.06 $J_{3,4}$ = 9.4	3.61	3.85	3.71
UDP-3-*O*-[(*R*)-3-hydroxymyristoyl]-GlcN	5.61 $J_{1,2}$ = 2.8 $J_{1,P}$ = 6.1	3.25 $J_{2,3}$ = 10.1	5.09 $J_{3,4}$ = 9.4	3.55	3.86	3.70
UDP-6-*O*-[(*R*)-3-hydroxymyristoyl]-GlcN	5.64	3.16	3.76	3.43	3.99	4.28
UDP-6-*O*-[(*R*)-3-hydroxymyristoyl]-GlcNAc	5.33	3.84	3.66	3.45	3.98	4.25

[a] Apparent center of AB pattern.

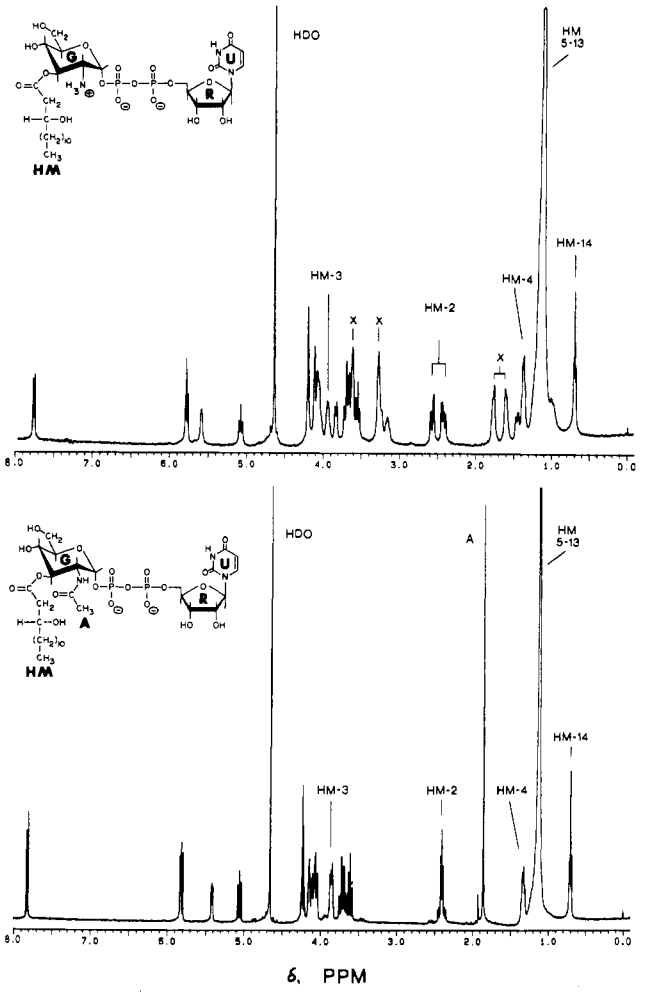

FIGURE 4: One-dimensional ^{1}H NMR analysis of putative UDP-3-*O*-[(*R*)-3-hydroxymyristoyl]glucosamine at 400 MHz. (Panel A) One-dimensional ^{1}H NMR spectrum of 2 mg of product, taken as described under Experimental Procedures. (Panel B) One-dimensional ^{1}H NMR spectrum obtained from a chemically synthesized sample (3 mg) of UDP-3-*O*-[(*R*)-3-hydroxymyristoyl]-GlcNAc. Both samples were exchanged twice with D_2O before acquisition of the spectra shown. Peaks marked with an "X" are contaminants derived from the membrane-free extracts used to prepare the sample. Abbreviations used refer to protons attached to carbons of the five domains of this molecule (boldface letters shown in the structure). These are HM, (*R*)-3-hydroxymyristate protons; A, acetyl protons; G, glucosamine ring protons; R, ribose ring protons; and U, uracil ring protons.

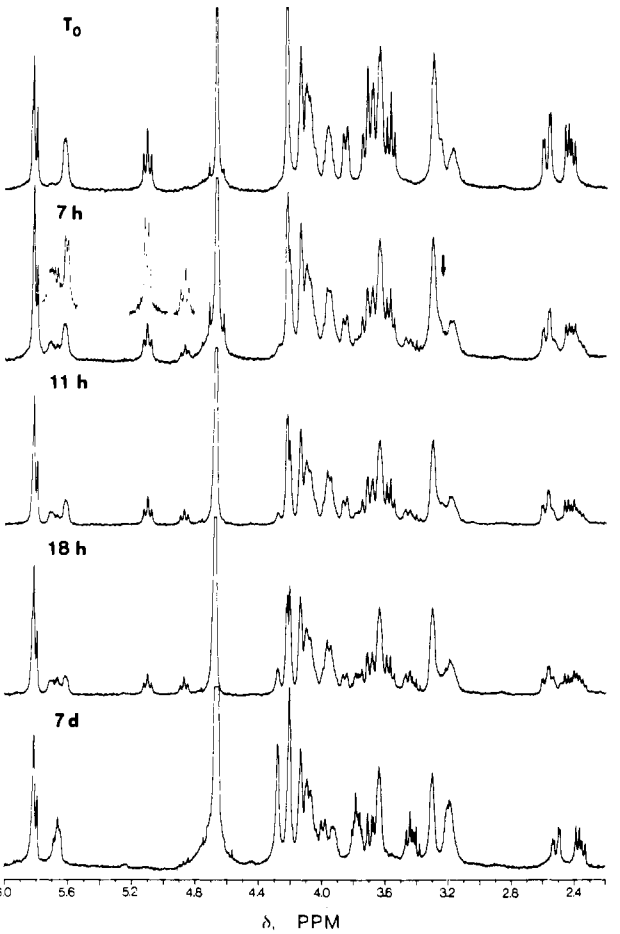

FIGURE 5: Expansion of the ^{1}H NMR spectrum of UDP-3-*O*-[(*R*)-3-hydroxymyristoyl]-GlcN and its change with time. This figure shows 400-MHz ^{1}H NMR spectra taken at various times as described under Experimental Procedures. Peak assignments are described in the text. At 7-h time, the G-2 proton of the glucosamine ring, identified in Figure 6A, was decoupled in a one-dimensional experiment to verify this assignment. Peak changes occurring as a result of this decoupling are shown.

group, we performed a two-dimensional COSY analysis of the putative UDP-3-*O*-[(*R*)-3-hydroxymyristoyl]-GlcN. The spectrum was acquired over a period of 7 hours and is shown in Figure 6A together with the corresponding one-dimensional spectrum. From the location of the anomeric glucosamine proton (G-1) at 5.61 ppm, one finds (from the single cross-peak) the shift of the glucosamine ring proton G-2 at 3.25 ppm, slightly obscured in the one-dimensional spectrum by signals from the impurities designated X in Figure 4. Similarly, on the G-2 vertical one finds the cross-peak between G-2 and G-3 at 5.09 ppm. The complete analysis of these data allows the assignment of the chemical shifts of all the glucosamine ring protons, as shown in Table I. The coupling constants in Table I were obtained by one-dimensional decoupling of the relevant peaks, as detailed below. Comparison of the glucosamine ring proton shifts in the putative UDP-3-*O*-[(*R*)-3-hydroxymyristoyl]-GlcN to those found in UDP-3-*O*-[(*R*)-3-hydroxymyristoyl]-GlcNAc shows evidence for two important structural features in the former. As shown previously for lipid X (2,3-diacyl-GlcN-1-P), acylation of a carbohydrate ring

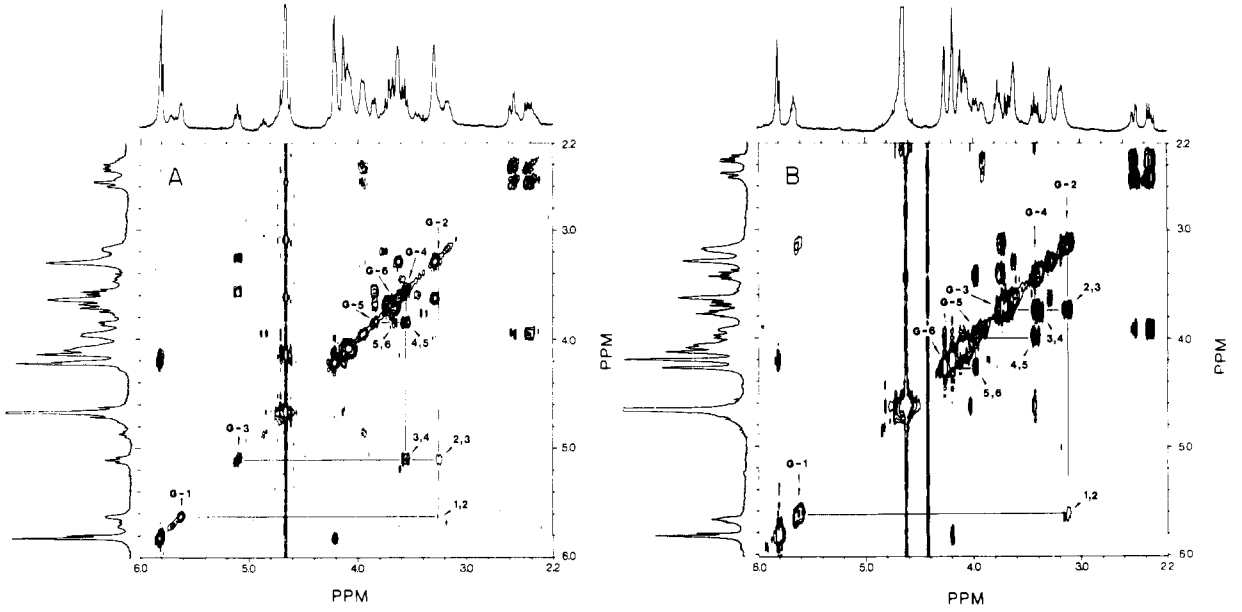

FIGURE 6: (Panel A) Two-dimensional COSY ^{1}H NMR analysis of UDP-3-*O*-[(*R*)-3-hydroxymyristoyl]-GlcN at 400 MHz. The spectrum was acquired in magnitude-calculated mode as described under Experimental Procedures. The region of the spectrum from 2.2 to 6.0 ppm is shown. Horizontal and vertical lines connect cross-peaks assigned to the glucosamine ring protons. These protons are identified according to the nomenclature described in Figure 4. (Panel B) Two-dimensional COSY ^{1}H NMR analysis at 400 MHz of the final rearrangement product formed from UDP-3-*O*-[(*R*)-3-hydroxymyristoyl]-GlcN. This spectrum was acquired after 7 days of rearrangement, in pure-absorption mode as described under Experimental Procedures. The scale of this spectrum and abbreviations used are identical with those shown in panel A.

hydroxyl causes a downfield shift of 1.2–1.5 ppm in the corresponding ring proton (Takayama et al., 1983a). The downfield shift of G-3 relative to its upfield position near 3.6 ppm in underivatized glucosamine indicates that this position is the site of fatty acylation in both the starting material and the product. A second important spectral feature of the product is the upfield shift of G-2 to 3.25 ppm from 4.05 ppm in the starting material. This is consistent with the presence of the positively charged amino group at position 2, following removal of the acetyl moiety.

FAB Mass Spectrometry of the Putative UDP-3-O-[(R)-3-hydroxymyristoyl]-GlcN. A portion of the material used for ^{1}H NMR spectroscopy was subjected to FAB mass spectrometry in the positive mode (Takayama et al., 1983a). Prominent peaks (data not shown) were observed at m/z 792 $(M + H)^+$, 814 $(M + Na)^+$, and 836 $(M - H + 2Na)^+$. The results support the conclusion that the acetyl moiety has been removed, since the starting material [UDP-3-*O*-[(*R*)-3-hydroxymyristoyl]-GlcN] has a chemical molecular weight of 833.72. The FAB mass spectrum of the product also revealed the presence of impurities, as judged by the presence of unidentified peaks of comparable height at m/z 1085 and 1107. Presumably, these impurities were introduced by the crude cytoplasmic fraction used as the source of deacetylase, and they may be related to the resonances designated X in Figure 4.

A Chemical Rearrangement of UDP-3-O-[(R)-3-hydroxymyristoyl]-GlcN Detected by ^{1}H NMR. Closer inspection of the spectrum of Figure 6A reveals several smaller signals that do not arise from UDP-3-*O*-[(*R*)-3-hydroxymyristoyl]-GlcN. Most notable of these are a new triplet at 4.86 ppm, extra signals appearing near 5.7 ppm, a set of peaks centered at 3.42 ppm, and increasing complication of the AB system around 2.42 ppm. The origin of these signals becomes clear when the one-dimensional spectrum taken at $T = 0$ (Figure 5) is compared to a 1-pulse one-dimensional spectrum taken at 7 h (Figure 5, second spectrum from the top). The new resonances appearing at 7 h strongly suggest chemical rearrangement of the sample. Consequently, additional spectra were acquired at later time points to examine this phenomenon further (Figure 5). One observes the diminution of the triplet at 5.09 ppm and a concomitant rise in new signals with time, indicating the movement of the (*R*)-3-hydroxymyristoyl moiety from the 3-position of the glucosamine ring to other locations. After 7 days, however, the spectrum simplified again and thereafter remained unchanged with time (Figure 5, bottom spectrum). At this point, the G-3 triplet at 5.09 ppm had disappeared completely with a concomitant increase in a new peak at 4.28 ppm. Interestingly, the AB system near 2.5 ppm was replaced with a nearly identical AB system, slightly upfield of the original, explaining the complexity of these signals at intermediate times when both forms are present. Also noteworthy is the time-dependent disappearance of the G-6 AB system centered at 3.7 ppm, the triplet at 3.55 ppm (identified as G-4 of the unrearranged material by the two-dimensional COSY analysis shown in Figure 6A), and the G-5 doublet of triplets at 3.86 ppm (Figure 5).

In order to determine where the (*R*)-3-hydroxymyristoyl moiety moved to, we performed another two-dimensional COSY analysis on the sample after 7 days (Figure 6B). The shifts of the glucosamine ring protons in this final product are given in Table I. The new resonance at 4.28 ppm arises from the G-6 protons, shifted downfield by 0.58 ppm relative to the starting material. The G-5 proton is shifted slightly downfield to 3.99 ppm, while the G-4 and G-2 protons are shifted slightly upfield relative to the starting material (Figure 5, $T = 0$ time point). As expected, the proton at the G-3 position, now unacylated, has moved upfield to 3.76 ppm. These data show that the site of acylation in the rearranged material is predominantly at the glucosamine G-6 hydroxyl group. The triplet that transiently appears at 4.86 ppm ($T = 7$, 11, and 18 h), and then disappears again ($T = 7$ days), has not been assigned unequivocally, but on the basis of its shape and coupling, it is likely to be the G-4 proton of glucosamine. The presence of the G-4 proton so far downfield strongly suggests that the G-4 hydroxyl is transiently acylated during migration

Table II: Composition (%) of *O*-Acyl Isomers Formed from UDP-3-*O*-[(*R*)-3-hydroxymyristoyl]-GlcN and UDP-3-*O*-[(*R*)-3-hydroxymyristoyl]-GlcNAc with Time

UDP-3-*O*-[(*R*)-3-hydroxymyristoyl]-GlcN			
time at 21 °C	H-3	H-4[a]	H-6
0	100	0	0
7 h	69	28	3
11 h	62	32	6
18.5 h	44	38	18
7 days	0	<5	>95

UDP-3-*O*-[(*R*)-3-hydroxymyristoyl]-GlcNAc			
time at 30 °C	H-3[b]	time at 30 °C	H-3[b]
0	100	28 h	55
9.5 h	79	8 days	29
22 h	60		

[a] Tentatively identified as described in the text. [b] Data obtained by 270-MHz ^{1}H NMR. An accurate determination of each of the 4- and 6-*O*-acyl isomers present was not possible in this case.

of the (*R*)-3-hydroxymyristoyl residue from position 3 to position 6.

We integrated the signals for several of these protons at all time points by cutting and weighting the peaks to determine the ratio of isomers. As shown in Table II, the fatty acyl moiety at position 3 of UDP-3-*O*-[(*R*)-3-hydroxymyristoyl]-GlcN disappears with a half-life of about 15 h at 21 °C, first presumably to position 4, and then to position 6. We cannot rule out the possibility that some migration from position 3 directly to position 6 may be occurring. However, the appearance of the putative 4-*O*-acyl isomer and its later disappearance suggests that the 3 to 4 to 6 route is predominant.

The acyl rearrangements described above for UDP-3-*O*-[(*R*)-3-hydroxymyristoyl]-GlcN were also observed to occur with UDP-3-*O*-[(*R*)-3-hydroxymyristoyl]-GlcNAc, but the latter rearranges 2–4 times more slowly with less accumulation of the putative 4-*O*-acyl intermediate. This was demonstrated by allowing the sample of UDP-3-*O*-[(*R*)-3-hydroxymyristoyl]-GlcNAc used to generate the ^{1}H NMR spectrum shown in the lower panel of Figure 4 to stand at 30 °C under conditions identical with those employed for the ^{1}H NMR analysis of the UDP-3-*O*-[(*R*)-3-hydroxymyristoyl]-GlcN (Figure 5). A two-dimensional COSY experiment at 400 MHz (data not shown) was carried out after 28 h to assign the newly appearing resonances. Chemical shifts of the glucosamine ring protons obtained from this analysis are summarized in Table I and indicate that the UDP-3-*O*-[(*R*)-3-hydroxymyristoyl]-GlcNAc had partially rearranged to give UDP-6-*O*-[(*R*)-3-hydroxymyristoyl]-GlcNAc as the major product and the putative 4-O-acylated isomer as the minor product. The percentage of the 3-*O*-acyl isomer remaining with time at 30 °C was also determined as shown in Table II.

Further Acylation and Metabolism of UDP-3-O-[(R)-3-hydroxymyristoyl]glucosamine. In order to prove that [β-^{32}P]UDP-3-*O*-[(*R*)-3-hydroxymyristoyl]-GlcN is a chemically and kinetically competent metabolite in the in vitro synthesis of UDP-2,3-diacyl-GlcN, we incubated this radiolabeled material with extracts in the presence of [(*R*)-3-hydroxymyristoyl]-ACP as described under Experimental Procedures. As shown in Figure 7 (lanes 2–5), ^{32}P-labeled UDP-2,3-diacyl-GlcN, 2,3-diacyl-GlcN-1-P, and tetraacyldisaccharide-1-P are formed with time from [β-^{32}P]UDP-3-*O*-[(*R*)-3-hydroxymyristoyl]-GlcN, in the expected order consistent with the pathway of Figure 1. A similar time course has previously been observed by starting with [β-^{32}P]UDP-3-*O*-[(*R*)-3-hydroxymyristoyl]-GlcNAc (Anderson & Raetz, 1987).

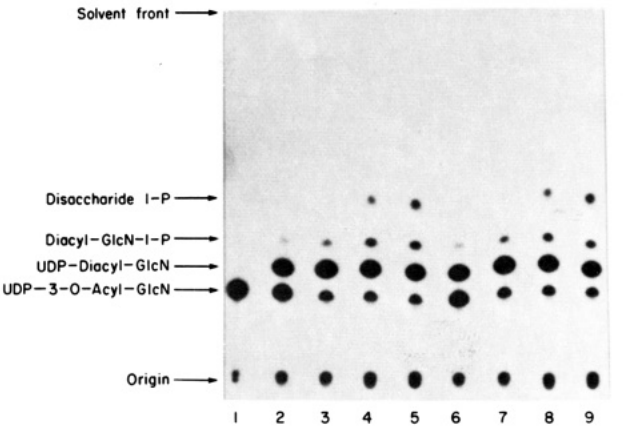

FIGURE 7: Enzymatic conversion of UDP-3-*O*-[(*R*)-3-hydroxymyristoyl]-GlcN to UDP-2,3-diacyl-GlcN and other lipid A precursors. This figure is an autoradiograph of a silica thin-layer plate developed in chloroform/methanol/water/acetic acid (25:15:4:2 v/v). The origin, solvent front, and the R_f's of various standards are indicated. With the exception noted, reaction mixtures contained 3.2 μM [β-^{32}P]-UDP-3-*O*-[(*R*)-3-hydroxymyristoyl]-GlcN (2×10^6 cpm/nmol), 100 μM [(*R*)-3-hydroxymyristoyl]-ACP, 40 mM HEPES, pH 8.0, and 0.8 mg/mL membrane-free extract from strain JB1104, prepared as described under Experimental Procedures. Portions of the reaction mixtures (5 μL) were spotted directly onto the plate at the times indicated. Lane 1, [β-^{32}P]UDP-3-*O*-[(*R*)-3-hydroxymyristoyl]-GlcN spotted directly onto the plate. Lanes 2–5, 2-, 5-, 15-, and 30-min time points, respectively, according to the conditions described above. Lanes 6–9, 2-, 5-, 15-, and 30-min time points, respectively, as above but with an extract that was preincubated at 0 °C for 30 min with 1 mM *N*-ethylmaleimide.

When the extract was pretreated at 0 °C for 30 min with 1 mM *N*-ethylmaleimide prior to assay, no significant change was observed in the rate of acylation of [β-^{32}P]UDP-3-*O*-[(*R*)-3-hydroxymyristoyl]-GlcN (Figure 7, lanes 6–9). This contrasts with the sensitivity of deacetylase to *N*-ethylmaleimide (Figure 2, lanes 6 and 12), suggesting that different active sites are involved in deacetylation and N-acylation.

Inspection of Figure 7 reveals the presence of a small amount of a radiolabeled material migrating with [β-^{32}P]-UDP-3-*O*-[(*R*)-3-hydroxymyristoyl]-GlcN, which is not further acylated or otherwise degraded. This ^{32}P-labeled material is likely to be the 4- and/or 6-*O*-acyl isomer of [β-^{32}P]UDP-*O*-[(*R*)-3-hydroxymyristoyl]-GlcN, which may have formed during the preparation of this compound. The level of this unreactive material increases with the age of the [β-^{32}P]-UDP-3-*O*-[(*R*)-3-hydroxymyristoyl]-GlcN. A similar phenomenon was previously observed with [β-^{32}P]UDP-3-*O*-[(*R*)-3-hydroxymyristoyl]-GlcNAc (Anderson & Raetz, 1987).

Detection of Acetate Release from UDP-3-O-[(R)-3-hydroxymyristoyl]-GlcNAc. In order to directly demonstrate the release of the acetate moiety from UDP-3-*O*-[(*R*)-3-hydroxymyristoyl]-GlcNAc during the formation of UDP-3-*O*-[(*R*)-3-hydroxymyristoyl]-GlcN, we incubated [*acetyl*-^{3}H]UDP-3-*O*-[(*R*)-3-hydroxymyristoyl]-GlcNAc with a membrane-free extract of JB1104 at pH 5.5 and separated the ^{3}H-labeled components by C18 reverse-phase HPLC as described under Experimental Procedures. A typical profile after a 15-min incubation is shown in Figure 8. In addition to the starting material, only one new peak of radioactivity, emerging at the position expected for acetic acid, is observed.

Discussion

We have recently reported the existence of a cytoplasmic enzyme in *E. coli* that acylates the 3-OH of the glucosamine ring of UDP-GlcNAc with an (*R*)-3-hydroxymyristoyl moiety (Anderson & Raetz, 1987). The resulting UDP-3-*O*-[(*R*)-

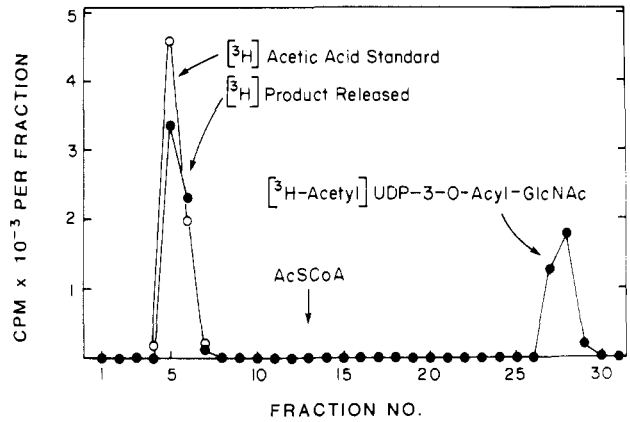

FIGURE 8: C18 reverse-phase HPLC analysis of all metabolites formed from [*acetyl*-^{3}H]UDP-3-*O*-[(*R*)-3-hydroxymyristoyl]-GlcNAc after 15 min. The Figure is a plot of the radioactivity found in each 1-mL fraction eluting off of a 5-μm C18 reverse-phase HPLC column, as described under Experimental Procedures. The position of standard acetyl coenzyme A (AcSCoA), monitored at 260 nm, is indicated by the arrow. The mobility of [^{3}H]acetic acid was determined in a separate experiment.

3-hydroxymyristoyl]-GlcNAc is both chemically and kinetically competent in the further generation of UDP-2,3-diacyl-GlcN (Anderson & Raetz, 1987), a minor *E. coli* lipid (Bulawa & Raetz, 1984a) that is crucial in the biosynthesis of the lipid A disaccharide.

Our efforts to clarify the steps involved in the transformation of UDP-3-*O*-[(*R*)-3-hydroxymyristoyl]-GlcNAc to UDP-2,3-diacyl-GlcN were aided by a lipase, present in membrane-free extracts of *E. coli*, that removes the (*R*)-3-hydroxymyristoyl moiety of UDP-3-*O*-[(*R*)-3-hydroxymyristoyl]-GlcNAc (Anderson & Raetz, 1987). This lipase also acted on UDP-3-*O*-[(*R*)-3-hydroxymyristoyl]-GlcN to form UDP-glucosamine, a compound that was easily detectable in our initial experiments. While this implicated the existence of UDP-3-*O*-[(*R*)-3-hydroxymyristoyl]-GlcN, the lipase also destroyed it very rapidly. Adjustment of the pH of the reaction mixture to 5.5 allowed us to inhibit the lipase selectively and to isolate sufficient quantities of the deacetylated product for spectroscopic analysis.

The presence of the lipase in *E. coli* extracts is intriguing. It may be an enzyme, unrelated to lipid A metabolism, that is fortuitously activated upon cell disruption. Alternatively, it may function to prevent the accumulation of UDP-3-*O*-[(*R*)-3-hydroxymyristoyl]-GlcNAc and UDP-3-*O*-[(*R*)-3-hydroxymyristoyl]-GlcN, both of which are likely to have the physical properties of detergents. In addition, we have shown that both 3-*O*-acyl nucleotides can rearrange to form 4- and 6-*O*-acyl isomers (Figure 9), which are metabolically inactive. It seems reasonable to believe that cells must guard against the accumulation of these biosynthetically inert products. Although UDP-3-*O*-[(*R*)-3-hydroxymyristoyl]-GlcNAc and UDP-3-*O*-[(*R*)-3-hydroxymyristoyl]-GlcN have not been isolated from living cells, Bulawa and Raetz (1984a) showed that UDP-2,3-diacyl-GlcN is the major uridine-labeled lipid of *E. coli* and is present at $\sim$100 molecules per cell in wild-type organisms.

Like UDP-3-*O*-[(*R*)-3-hydroxymyristoyl]-GlcNAc, UDP-3-*O*-[(*R*)-3-hydroxymyristoyl]-GlcN is quickly converted to UDP-2,3-diacyl-GlcN upon incubation with *E. coli* extracts and the acyl donor, [(*R*)-3-hydroxymyristoyl]-acyl carrier protein. The sensitivity of the deacetylation step to *N*-ethylmaleimide, in contrast to the subsequent N-acylation reaction, suggests that two distinct active sites are involved. Since the extract has not been fractionated, the question of

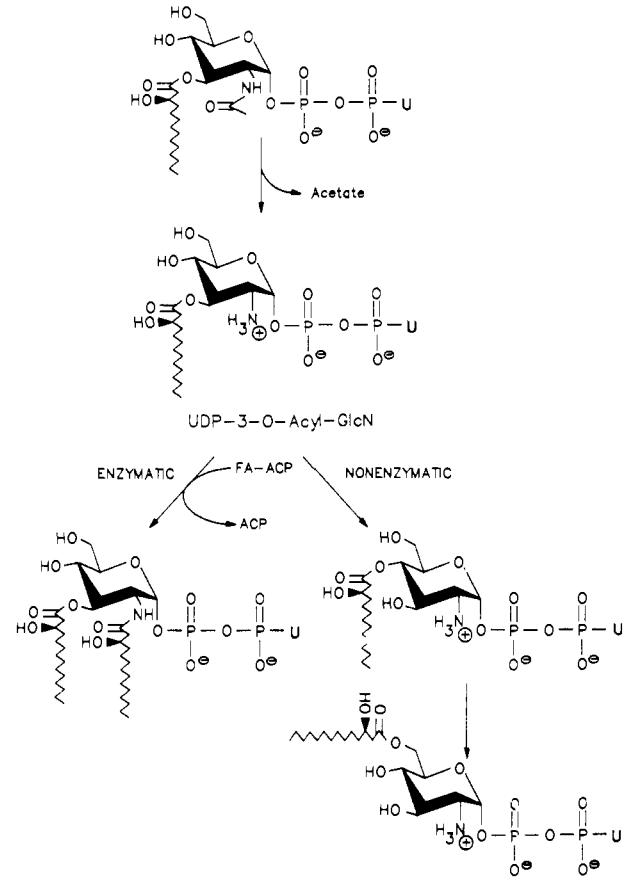

FIGURE 9: Biosynthesis of UDP-3-*O*-[(*R*)-3-hydroxymyristoyl]-GlcN in *E. coli* and its subsequent enzymatic or nonenzymatic transformations. Data presented in this study indicate that the lipid A precursor UDP-2,3-diacyl-GlcN is formed from UDP-3-*O*-[(*R*)-3-hydroxymyristoyl]-GlcNAc by an initial deacetylation to generate UDP-3-*O*-[(*R*)-3-hydroxymyristoyl]-GlcN. In the presence of an appropriate acyl donor and enzyme this material is rapidly acylated to UDP-2,3-diacyl-GlcN. Alternatively, nonenzymatic rearrangement to 4- and 6-*O*-acyl isomers can occur in aqueous solution. The UDP-3-*O*-[(*R*)-3-hydroxymyristoyl]-GlcNAc can undergo a similar, nonenzymatic rearrangement (not shown), but at a rate that is 2–4 times slower.

whether UDP-3-*O*-[(*R*)-3-hydroxymyristoyl]-GlcNAc is deacetylated and, subsequently, N-acylated by two separable enzymes or by a single, bifunctional protein remains unanswered.

Enzymatic deacetylation of substituted GlcNAc residues is not entirely without precedent in metabolism. In animal cells, GlcNAc residues of heparan sulfate are deacetylated prior to N-sulfation (Höök, 1984). Little is known about the structure and function of these enzymes.

The disaccharide backbone of mature lipid A is acylated with four (*R*)-3-hydroxymyristoyl moieties, situated at positions 2, 3, 2′, and 3′ (Rietschel, 1984). We have previously shown that the UDP-GlcNAc acyltransferase of *E. coli* is absolutely specific in the transfer of an (*R*)-3-hydroxymyristoyl moiety, activated by acyl carrier protein, to the 3-position of the glucosamine ring, accounting for the specificity of fatty acid placement at positions 3 and 3′ of mature lipid A, as shown in Figure 1 (Anderson & Raetz, 1987). We now believe that the fatty acids attached to positions 2 and 2′ of lipid A are incorporated by the *N*-acyltransferase, described here. Unlike UDP-GlcNAc acyltransferase, however, the *N*-acyltransferase functions with palmitoyl-acyl carrier protein as the acyl group donor, albeit much more slowly than with [(*R*)-3-hydroxymyristoyl]-acyl carrier protein (Anderson & Raetz, 1987). N-Linked palmitoyl moieties have not been detected

in mature lipid A of *E. coli* (Rietschel, 1984). The *N*-acyltransferase of lipid A metabolism might have some similarities to the poorly characterized, eucaryotic *N*-acyltransferases involved in ceramide biosynthesis (Sweeley, 1985) or protein myristoylation (Kamps et al., 1985).

In summary, we believe that the formation of UDP-2,3-diacyl-GlcN from UDP-3-*O*-[(*R*)-3-hydroxymyristoyl]-GlcNAc proceeds under our in vitro conditions by removal of acetate followed by the addition of an (*R*)-3-hydroxymyristoyl group to the amino function, as shown in Figure 9. However, we cannot rule out the possibility of still other biosynthetic routes to UDP-2,3-diacyl-GlcN in living cells, until mutants, specifically defective in the enzymes that we have discovered, are available.

ACKNOWLEDGMENTS

We thank Dr. Laurens Anderson for many helpful discussions. This study made use of the National Magnetic Resonance Facility at Madison, which is supported in part by NIH Grant RR02301 from the Biomedical Research Technology Program, Division of Research Resources. Equipment in the facility was purchased with funds from the University of Wisconsin, the NSF Biological Instrumentation Program (Grant PCM-845048), the NIH Shared Instrumentation Program (Grant RR02301), and the U.S. Department of Agriculture.

REFERENCES

Anderson, M. S., & Raetz, C. R. H. (1987) *J. Biol. Chem. 262*, 5159–5169.

Anderson, M. S., Bulawa, C. E., & Raetz, C. R. H. (1985) *J. Biol. Chem. 260*, 15536–15541.

Bax, A., & Freeman, R. (1981) *J. Magn. Reson. 44*, 542–561.

Bulawa, C. E., & Raetz, C. R. H. (1984a) *J. Biol. Chem. 259*, 4846–4851.

Bulawa, C. E., & Raetz, C. R. H. (1984b) *J. Biol. Chem. 259*, 11257–11264.

Crowell, D. N., Anderson, M. S., & Raetz, C. R. H. (1986) *J. Bacteriol. 168*, 152–159.

Galanos, C., Lüderitz, O., Rietschel, E. Th., & Westphal, O. (1977) in *International Review of Biochemistry: Biochemistry of Lipids II* (Goodwin, T. W., Ed.) Vol. 14, pp 239–335, University Park Press, Baltimore.

Galanos, C., Freudenberg, M. A., Lüderitz, O., Rietschel, E. Th., & Westphal, O. (1979) in *Biomedical Application of the Horseshoe Crab (Limulidae)* (Cohen, E., Ed.) pp 321–332, Liss, New York.

Hinshaw, L. B., Ed. (1984) *Handbook of Endotoxin, Pathophysiology of Endotoxin*, Vol. 2, Elsevier, Amsterdam.

Höök, M., Kjellén, L., & Johansson, S. (1984) *Annu. Rev. Biochem. 53*, 847–869.

Imoto, M., Kusumoto, S., Shiba, T., Naoki, H., Iwashita, T., Rietschel, E. Th., Wollenweber, H.-W., Galanos, C., & Lüderitz, O. (1983) *Tetrahedron Lett. 24*, 4017–4020.

Inage, M., Chaki, H., Kusumoto, S., & Shiba, T. (1982) *Chem. Lett.*, 1281–1284.

Kamps, M. P., Buss, J. E., & Sefton, B. M. (1985) *Proc. Natl. Acad. Sci. U.S.A. 82*, 4625–4628.

Kenner, G. W., Todd, A. R., & Weymouth, F. J. (1952) *J. Chem. Soc.*, 3675–3681.

Lang, L., & Kornfeld, S. (1984) *Anal. Biochem. 140*, 264–269.

Macher, I. (1987) *Carbohydr. Res. 162*, 79–84.

Marion, D., & Wüthrich, K. (1983) *Biochem. Biophys. Res. Commun. 113*, 967–974.

Morrison, D. C., & Ryan, J. L. (1979) *Adv. Immunol. 28*, 293–450.

Nishijima, M., & Raetz, C. R. H. (1979) *J. Biol. Chem. 254*, 7837–7844.

Patterson, M. S., & Green, R. C. (1965) *Anal. Biochem. 37*, 856–862.

Peterson, G. L. (1977) *Anal. Biochem. 83*, 346–356.

Qureshi, N., Takayama, K., Heller, D., & Fenselau, C. (1983) *J. Biol. Chem. 258*, 12947–12951.

Raetz, C. R. H. (1986) *Annu. Rev. Genet. 20*, 253–295.

Ray, B. L., Painter, G., & Raetz, C. R. H. (1984) *J. Biol. Chem. 259*, 4852–4859.

Rietschel, E. Th., Ed. (1984) *Handbook of Endotoxin, Chemistry of Endotoxin*, Vol. 1, Elsevier, Amsterdam.

Rietschel, E. Th., Wollenweber, H.-W., Sidorczyk, Z., Zähringer, U., & Lüderitz, O. (1983) in *Bacterial Lipopolysaccharides. Structure, Synthesis, and Biological Activities* (Anderson, L., & Unger, F. M., Eds.) ACS Symp. Ser. No. 231, p 214, American Chemical Society, Washington, DC.

Rock, C. O., & Cronan, J. E., Jr. (1980) *Anal. Biochem. 102*, 362–364.

Roth, W., & Pigman, W. (1960) *J. Am. Chem. Soc. 82*, 4608–4611.

Strain, S. M., Fesik, S. W., & Armitage, I. M. (1983) *J. Biol. Chem. 258*, 2906–2910.

Sweeley, C. (1985) in *Biochemistry of Lipids and Membranes* (Vance, D. E., & Vance, J. E., Eds.) pp 361–403, Benjamin/Cummings, Menlo Park, CA.

Takayama, K., Qureshi, N., Mascagni, P., Nashed, M. A., Anderson, L., & Raetz, C. R. H. (1983a) *J. Biol. Chem. 258*, 7379–7385.

Takayama, K., Qureshi, N., & Mascagni, P. (1983b) *J. Biol. Chem. 258*, 12801–12803.

Takayama, K., Qureshi, N., Mascagni, P., Anderson, L., & Raetz, C. R. H. (1983c) *J. Biol. Chem. 258*, 14245–14252.

Wider, G., Macura, S., Kumar, A., Ernst, R. R., & Wüthrich, K. (1984) *J. Magn. Reson. 56*, 207–234.